ACS APPLIED MATERIALS & INTERFACES

Research Article

www.acsami.org

Selective Tuning of Gilbert Damping in Spin-Valve Trilayer by Insertion of Rare-Earth Nanolayers

Wen Zhang,*[,†,‡] Dong Zhang,[†] Ping Kwan Johnny Wong,[§,∥] Honglei Yuan,[†] Sheng Jiang,[†] Gerrit van der Laan,[⊥] Ya Zhai,*[,†] and Zuhong Lu[‡]

[†]Department of Physics, Southeast University, Nanjing 211189, China

[‡]School of Biological Sciences & Medical Engineering, Southeast University, Nanjing 210096, China

[§]Department of Chemistry, National University of Singapore, 3 Science Drive 3, Singapore 117543

[∥]NanoElectronics Group, MESA+ Institute for Nanotechnology, University of Twente, 7500 AE Enschede, The Netherlands

[⊥]Magnetic Spectroscopy Group, Diamond Light Source, Didcot OX11 0DE, United Kingdom

ABSTRACT: Selective tuning of the Gilbert damping constant, α, in a NiFe/Cu/FeCo spin-valve trilayer has been achieved by inserting different rare-earth nanolayers adjacent to the ferromagnetic layers. Frequency dependent analysis of the ferromagnetic resonances shows that the initially small magnitude of α in the NiFe and FeCo layers is improved by Tb and Gd insertions to various amounts. Using the element-specific technique of X-ray magnetic circular dichroism, we find that the observed increase in α can be attributed primarily to the orbital moment enhancement of Ni and Co, rather than that of Fe. The amplitude of the enhancement depends on the specific rare-earth element, as well as on the lattice and electronic band structure of the transition metals. Our results demonstrate an effective way for individual control of the magnetization dynamics in the different layers of the spin-valve sandwich structures, which will be important for practical applications in high-frequency spintronic devices.

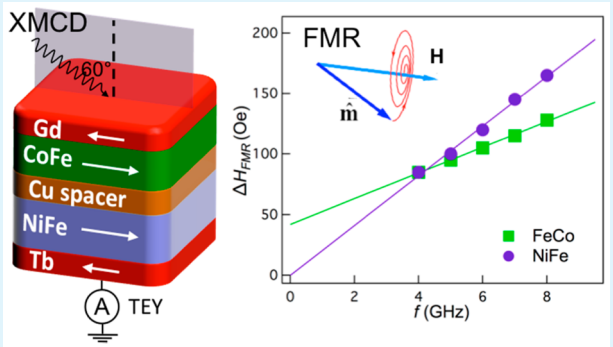

KEYWORDS: *spintronics, ferromagnet/normal-metal/ferromagnet trilayer, rare-earths, Gilbert damping, spin−orbit coupling, orbital moment, FMR, XMCD*

INTRODUCTION

As an essential building block to spin-valves, ferromagnet/normal-metal/ferromagnet hybrid structures have received tremendous attention over the last two decades.[1,2] In such trilayer structures, the magnetizations in the two ferromagnetic layers are effectively decoupled by a normal-metal spacer, which in turn can be switched individually by an external magnetic field.[3,4] As a result, the electrical resistance of the trilayers depends on the relative alignment of the static magnetizations in the ferromagnetic layers. This well-documented phenomenon is referred to as the spin-valve effect.[5−7] One of the present-day major research efforts of the spintronics community has been focusing on more advanced applications of these spin-valve trilayers in high-frequency spintronic devices, such as spin-torque oscillators (STO),[8] spin-torque transistors,[9] microwave generators,[10] etc. These devices take advantage of the dynamic interplay between the local magnetization and the spin-polarized current,[11] which is fundamentally governed by the Gilbert damping in the trilayer. The Gilbert damping constant α is an intrinsic parameter that has been experimentally related to the orbital magnetic moment[12] and characterizes the magnetization dynamics,[13] such as the magnetic relaxation and switching behavior in ferromagnetic materials. In the aforementioned applications that are based on spin-valves, the relative strength of α in each ferromagnetic layer becomes highly critical, due to their mutual influence.[14−16] A distinct example in this regard is a new type of STO, composed of two perpendicular polarizers at the two poles and two in-plane free layers with a normal-metal spacer in between, which is expected to enable the generation of an extraordinary large microwave power at frequencies higher than those attainable in STOs with a single polarizer and single free layer.[17] The spin-valve trilayer structure, containing the two free layers and the spacer, constitutes the crucial part in this type of STO, and more importantly, precise manipulation over the dynamic damping in the spin-valve structure plays a key role in the overall performance of such a device.[17] Motivated by this, our present work focuses on realizing the effective tuning of the individual Gilbert damping in each ferromagnetic layer of the spin-valve trilayers,[18−20] which could be applicable to a broader range of high-frequency spintronic devices as well, e.g., the

Received: April 25, 2015
Accepted: July 16, 2015
Published: July 16, 2015

DOI: 10.1021/acsami.5b03595
ACS Appl. Mater. Interfaces 2015, 7, 17070−17075

proposed spin batteries with pure spin transport in the spin-valve trilayer driven by ferromagnetic resonance.[21]

Although conceptually intriguing, a realistic control of the individual damping in each ferromagnetic layer is challenging. This is partly because α in 3*d* transition-metal (TM) ferromagnets is usually quite small, due to the quenched orbital magnetic moments and therefore small effective spin−orbit coupling in the materials.[22] There exists some experimental studies, showing a considerable enhancement in α by incorporating unusual dopants with a large orbital moment, such as rare-earth (RE) atoms with localized 4*f* electrons.[23−28] However, several undesirable issues for device application, apart from distortion or alteration of the crystal structure of the ferromagnets, may be caused by the dopants: For instance, soft magnetism is preferred in magnetic domain wall devices to allow to tailor their behavior via shape anisotropy, whereas the RE dopants may result in a deterioration of the soft magnetic properties of the ferromagnets under investigation.[29−31] On the other hand, RE dopants may lead to a strong perpendicular magnetic anisotropy in some specific situations,[32−34] which excludes such a doping method to be used in the context of STOs with dual in-plane free layers[17] as well as some lateral spintronic devices. Alternatively, other reports have suggested to utilize RE capping layers grown on top of ferromagnets, in which case not only could the magnetic moments of the ferromagnets mostly be maintained but the adverse effects of the RE dopants on the magnetoresistance of the ferromagnets could also be avoided.[35,36] This has stimulated our idea of inserting RE nanolayers adjacent to the ferromagnets, as presented in this work.

Here, we report a major step forward by exploiting the insertion of RE nanolayers in a NiFe/Cu/FeCo spin-valve trilayer. We demonstrate, by means of ferromagnetic resonance (FMR) and X-ray magnetic circular dichroism (XMCD), that selective adjustment of α in each ferromagnetic layer of the spin-valve is practically realizable by using various combinations of RE and 3*d* ferromagnetic layers, and also present for the first time a rule, at the atomic level, for how to obtain a desired or required Gilbert damping in spin-valve trilayers.

EXPERIMENTAL SECTION

Two stacks of spin-valve multilayers were deposited on silicon substrates at room temperature by magnetron sputtering under a base pressure of 1.0×10^{-5} Pa. The structures are schematically displayed in Figure 1a, where stack A is composed of Ta(5)/$Ni_{80}Fe_{20}$(3)/Cu(1.4)/$Fe_{50}Co_{50}$(2.5)/Ta(1) and stack B is Ta(5)/Tb(0.5)/$Ni_{80}Fe_{20}$(3)/Cu(1.4)/$Fe_{50}Co_{50}$(2.5)/Gd(0.5)/Ta(1) (all thicknesses in nm). NiFe and FeCo are among the most commonly used ferromagnetic layers for spin-valve structures, and Cu is adopted as the intermediate nonmagnetic interlayer to decouple the two ferromagnetic layers. In stack B, RE nanolayers of Tb and Gd were deposited adjacent to the NiFe and FeCo layers, respectively. Such a structural design enables XMCD studies of the effects of each of the magnetic layers, which possess at least one unique element distinguished from those in the other layers. Ta was used both as buffer and capping layer, where the latter was kept as thin as 1 nm in order to enable the XMCD detection of the layers underneath. During growth, a magnetic field of 50 Oe was applied to induce a small in-plane uniaxial anisotropy in the stacks.

Static magnetic properties were characterized using vibrating sampling magnetometry (VSM), whereas dynamical magnetic properties were investigated by FMR measurements. FMR spectra were obtained by recording the relative susceptibility as a function of the applied magnetic field, in a microwave frequency range of 4−9 GHz. The damping parameter of each ferromagnetic layer in the stacks was extracted using the frequency dependence of the FMR linewidth. X-ray absorption spectroscopy (XAS) and XMCD were carried out utilizing 90% circularly polarized X-rays on beamline I1011 at MAX-Laboratory in Lund, Sweden. The spectra were collected in total-electron-yield mode, in which the sample drain current is recorded as a function of the photon energy. The angle of incidence of the X-ray beam was set to 60° relative to the sample surface normal, as shown in Figure 1a. All measurements were taken at room temperature.

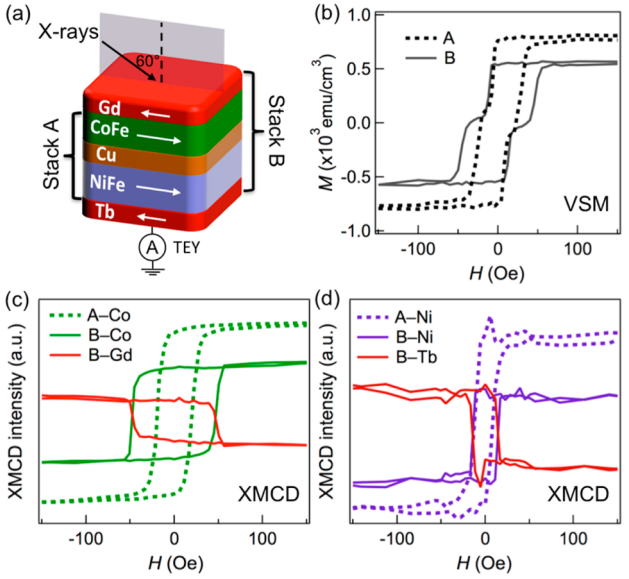

Figure 1. (a) Schematic structure for stacks A and B, and the XMCD measurement geometry. (b) Hysteresis loops of stack A (black dashed line) and stack B (black solid line) taken by VSM, with the applied magnetic field along the easy axis of the induced uniaxial anisotropy in the film plane. (c, d) Element-specific hysteresis loops for Co (green), Gd (red), Ni (purple), and Tb (firebrick) taken by XMCD, for stack A (dashed lines) and stack B (solid lines).

RESULTS AND DISCUSSION

Figure 1b shows the hysteresis loops of both stacks taken by VSM, with the magnetic field applied in the film plane, along the easy axis of the small induced uniaxial anisotropy. All loops display a two-step-switching behavior, suggesting a magnetic decoupling of the two TM layers by the Cu spacer. Two coercivity (H_C) values of each loop are obtained, corresponding to the NiFe (lower, $H_{C,NiFe}$) and FeCo (higher, $H_{C,FeCo}$) layers. By comparing the loops of stacks A and B, we found that upon insertion of the Tb and Gd layers, the magnitudes of $H_{C,NiFe}$ and $H_{C,FeCo}$ both increase but to a different extent, as summarized in Table 1, accompanied by a decrease in saturation magnetization (M_S). More precisely, the increase in $H_{C,NiFe}$ is ∼36%, which is much lower than that in $H_{C,FeCo}$ of 125%. This leads to an enhanced difference between the two

Table 1. Saturation Magnetization (M_S) and Coercivity (H_C) of Stack A (NiFe/Cu/FeCo) and stack B (Tb/NiFe/Cu/FeCo/Gd), Respectively

	stack A	stack B
M_S (emu/cm^3)	800	559
$H_{C,NiFe}$ (Oe)	11	15
$H_{C,FeCo}$ (Oe)	20	45
α_{NiFe} ($\times 10^{-2}$)	0.68	2.95
α_{FeCo} ($\times 10^{-2}$)	0.71	1.48

DOI: 10.1021/acsami.5b03595
ACS Appl. Mater. Interfaces 2015, 7, 17070−17075

coercivity values and consequently a much more distinct character of the two-step switching.

Element-specific hysteresis loops, monitored by XMCD, reveal the magnetization process of each layer, as shown in Figure 1c, d. In agreement with the results of the VSM loops, the coercivities for Co and Ni are very close to the values of $H_{C,FeCo}$ and $H_{C,NiFe}$. Most importantly, it was found that in stack B, the Gd aligns opposite to the Co moment, and so does the Tb to the Ni moment. This demonstrates an antiferromagnetic coupling between the TM and RE nanolayers, and consequently explains the reduction in M_S and enhancement in H_C, suggesting that the very thin layers of RE have sufficiently modified the magnetic properties of the system. Note that due to the finite probe depth of XMCD, the Tb/NiFe layers underneath show a lower signal-to-noise ratio compared to the top layers of FeCo/Gd, as is also seen from the XMCD spectra.

To obtain the Gilbert damping constants, α, we carried out FMR measurements over a microwave frequency range of 4−9 GHz. These frequency dependent measurements allow us to assess the FMR linewidth (ΔH) as a function of frequency (f) and thus to distinguish the Gilbert damping from other contributions, such as two-magnon scattering and sample inhomogeneity.[37] Figure 2a shows the typical FMR spectra for

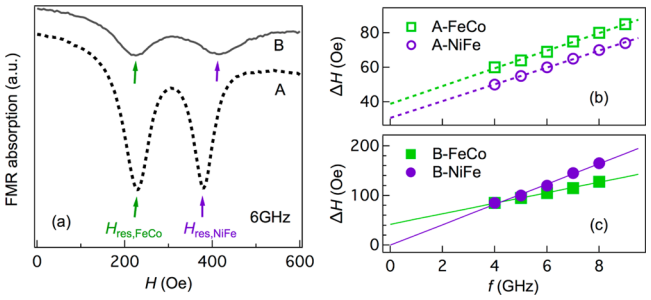

Figure 2. (a) Typical FMR absorption for stacks A and B, measured at a microwave frequency f = 6 GHz, as a function of the applied magnetic field in the film plane. (b, c) FMR linewidth ΔH for each of the two resonances of stack A (open symbols) and stack B (closed symbols), respectively, as a function of f. The straight lines are linear fits to the data points.

both stacks at 6 GHz. The spectra exhibit two resonance peaks corresponding to the FeCo and NiFe layers, respectively, as marked by arrows. Comparing the resonances of stack A and B, we notice that upon RE insertion, the separation between the resonance fields is increased, together with the peak broadening, which implies increased linewidths for both FeCo and NiFe.

The frequency dependence of the linewidths is plotted in Figure 2b-c, showing a linear behavior for both FeCo and NiFe in each stack. Therefore, the relationship between ΔH and f can be simply expressed as $\Delta H(f) = \Delta H(0) + (2\pi f/\gamma)\alpha$,[38] where $\Delta H(0)$ is the zero-frequency intercept caused by structural imperfections[39,40] and γ is the gyromagnetic ratio. The Gilbert damping constants, α, extracted from the slope of the linear fitting of $\Delta H(f)$ are summarized in Table 1. From this table we see that after Tb and Gd insertion the Gilbert damping constants α_{NiFe} and α_{FeCo} are separately improved to about four and two times their original values, respectively. The present result shows that the Gilbert damping in the NiFe and FeCo layers has been individually modified by Tb and Gd nanolayers, and their values, initially small and similar to each other in stack A, have been adjusted to a relationship of $\alpha_{NiFe} \approx 2\alpha_{FeCo}$ in stack B. This demonstrates the possibility of selectively engineering the Gilbert damping in different layers by inserting various types of RE, wherever needed, into the spin-valve trilayers.

To find out the mechanism behind the improved Gilbert damping and in turn a rule for obtaining controllable damping in different layers, we performed element-specific XMCD, which is an ideal tool to study the influence of the spin−orbit coupling because of its unique capability to separate the orbital and spin moments.[41,42] Figure 3a−c shows the normalized

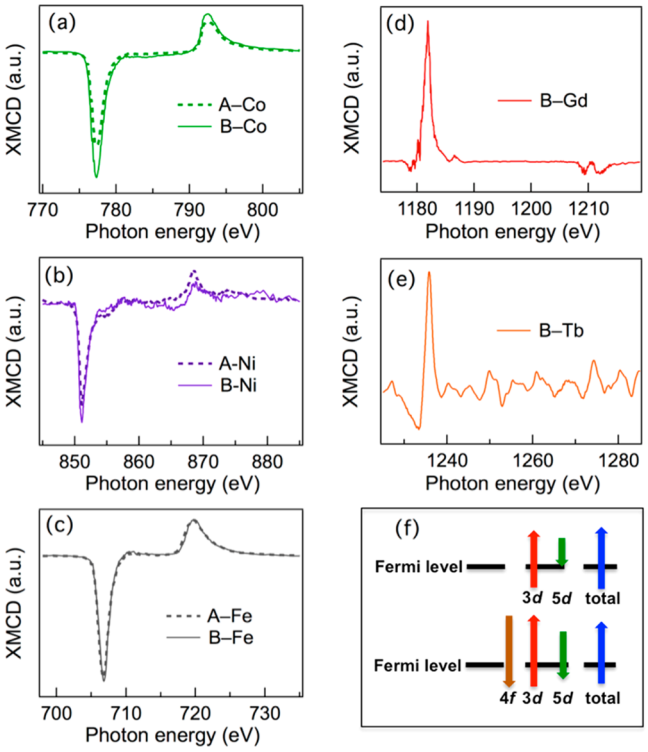

Figure 3. (a−c) XMCD spectra taken at the Co, Ni, and Fe $L_{2,3}$ edges, respectively, for stack A (dashed line) and stack B (solid line). (d−e) XMCD spectra taken at the Gd and Tb $M_{4,5}$ edges, respectively, for stack B. (f) Schematic picture of the spin contributions of the TM 3d and RE 5d states without 4f states (top panel) and with 4f states (bottom panel).

XMCD spectra for the TM (Co, Ni, and Fe) $L_{2,3}$ edges, taken in the remnant state of the samples after magnetic saturation, from which the orbital (m_L) and spin (m_S) moments of the TMs can be evaluated using the sum rules analysis.[43,44] The spectra at the RE (Gd and Tb) $M_{4,5}$ edges in stack B are also examined, and shown in Figure 3d, e, exhibiting an antiferromagnetic coupling to the TMs, as was already demonstrated by the XMCD loops in Figure 1c, d.

Table 2 summarizes the results for the m_L and m_S values extracted from the TM spectra, together with their ratios (m_L/m_S) and the total magnetic moments (m_L+m_S). As an important factor to evidence the influence of the spin−orbit coupling, the m_L/m_S ratio displays an interesting variation upon RE insertion. Namely, the m_L/m_S ratios for Co and Ni show an apparent increase of 37.5% and 123%, respectively, after inserting the Gd and Tb nanolayers, while for Fe this ratio shows nearly no change. This suggests that the improved Gilbert damping in stack B mainly arises from the enhanced orbital moments of Co

DOI: 10.1021/acsami.5b03595
ACS Appl. Mater. Interfaces 2015, 7, 17070−17075

Table 2. Orbital (m_L) and Spin (m_S) Moments (in units of μ_B/atom) of Co, Ni, and Fe in Stack A and Stack B, Respectively, Extracted from the XMCD Spectra Using the Sum Rules[a]

element	moments	stack A	stack B	relative increase (%)
Co	m_L	0.19 ± 0.03	0.29 ± 0.04	52.6
	m_S	1.21 ± 0.18	1.32 ± 0.20	9.1
	m_L+m_S	1.40 ± 0.18	1.61 ± 0.20	15
	m_L/m_S	0.16 ± 0.03	0.22 ± 0.05	37.5
Ni	m_L	0.07 ± 0.01	0.16 ± 0.02	129
	m_S	0.53 ± 0.08	0.55 ± 0.08	3.8
	m_L+m_S	0.60 ± 0.08	0.71 ± 0.08	18.3
	m_L/m_S	0.13 ± 0.03	0.29 ± 0.06	123
Fe	m_L	0.18 ± 0.03	0.19 ± 0.03	5.5
	m_S	1.76 ± 0.26	1.78 ± 0.27	1.1
	m_L+m_S	1.94 ± 0.26	1.97 ± 0.27	1.5
	m_L/m_S	0.10 ± 0.02	0.11 ± 0.02	10

[a]The last column gives the relative increase of the values after RE nanolayer insertions.

and Ni, whereas Fe shows little response to the RE and consequently only gives a tiny effect in damping improvement.

Concerning the spin moments of Co, Ni, and Fe, all of them were found to increase with RE insertion, although the augmentation is very small. The underlying mechanism for this is illustrated in Figure 3f.[45] In RE-TM compounds, the TM 3*d* orbitals are hybridized with the RE 5*d* orbitals with an antiferromagnetic coupling between the spins. The localized RE 4*f* electrons couple parallel to the RE 5*d* spins, so that the resulting indirect 4*f*−3*d* exchange coupling is antiferromagnetic.[46] This mechanism also holds for RE-TM interface layers, such as the Tb/NiFe and FeCo/Gd interfaces, but here it results in a damped oscillatory behavior of the moments as a function of distance, as has been demonstrated by X-ray resonant reflectivity measurements[47] and ab initio calculations using relativistic local spin density theory.[48] In Figure 3f, the top panel illustrates the antiparallel alignment between TM 3*d* and RE 5*d* spins (in the absence of 4*f* states) resulting from the hybridization between both states. When there is a localized 4*f* spin, the conduction electron spins between the RE and TM sites are redistributed, leading to an increase in 3*d* spin-down holes. Correspondingly, the 3*d* spin moment, which is equal to the numbers of spin-down minus spin-up holes, is increased as well. As shown in Figure 3f, in the presence of the localized 4*f* spin, both the 3*d* and 5*d* spin moments increase, whereas the total moment remains constant, which explains the observed increase in the 3*d* spin moments of Co, Fe, and Ni.

Remarkably, the observed increase of m_L is much more pronounced than that of m_S. Upon the RE insertions, the m_L of Co and Ni increase by 52.6% and 129%, respectively, which corresponds to a large enhancement in their m_L/m_S ratios. Compared to Co, the higher increase in m_L for Ni is consistent with the greater improvement for α_{NiFe} than for α_{FeCo}. In Tb this effect is reinforced by an orbital 4*f* contribution parallel to the spin, because the 4*f* shell is more than half-filled, while Gd lacks a 4*f* orbital moment, so that Tb has a more profound effect on facilitating the spin−orbit coupling in the adjacent NiFe.[49−51] In contrast, the m_L of Fe shows a very modest increase of 5.5%. The drastic difference between Fe and the other two (Co and Ni) suggests that in addition to the influence of the RE nanolayer, the orbital moment of the TM also depends on the lattice structure and the electronic band structure. Specifically, the orbital moment depends strongly on the details of the occupied and unoccupied states near the Fermi level.[52] If the position of the Fermi level shifts, as happens when the spin moment changes, then also the orbital moment will change. Although m_L strongly depends on the electronic structure, some general trends can be noted. Because $m_L = 0$ for completely filled and empty spin bands, m_L should reach a maximum value for a half-filled spin-down band. This means that the change in m_L would be the largest for one-quarter and three-quarter filled spin bands. Fe with $m_S = 1.76$ μ_B is approaching a half filled spin-down band and is in a region where the orbital moment is rather constant, hence the change in m_L with increasing number of 3*d* spin-down holes will be small. This is opposite to Ni, with $m_S = 0.53$ μ_B, where increasing the number of 3*d* holes results in a large change in m_L. Co is a more special case as $Fe_{50}Co_{50}$ has a large magnetic anisotropy, which is the reason that its m_L is enhanced compared to that of Fe or Ni metal. For the three-quarter filled spin band of Co, with $m_S = 1.21$ μ_B, a large increase in m_L can be expected when the number of 3*d* holes increases.

From the above, a simple rule can be formulated for selective control of the damping in a trilayer: To acquire a large magnitude of α, RE metals with relatively large orbital moment should be selected, e.g., Dy, Ho, Er, or Tm. At the same time, TMs with nearly three-quarter filled spin bands are promising, which can give a strong response to the RE insertion in their orbital moment and therefore tend to have a strong enhancement in the damping, such as Ni- and Co-rich alloys. On the other hand, if a relatively moderate Gilbert damping is desirable, RE with small or no orbital moment (Gd) and Fe or Fe-rich alloys might be suitable candidates. In other words, various combinations of RE and TM layers offer different kinds of possibilities to engineer the Gilbert damping for diverse demands. Finally, because of the increase in both m_L and m_S of the TMs after RE insertion, the total magnetic moment also increases, indicating that the magnetic moments in the TM layers have not been diluted but are actually improved by the RE.

CONCLUSIONS

In summary, we have provided an effective method to selectively engineer the Gilbert damping constants in a NiFe/Cu/FeCo spin-valve trilayer, by inserting nanolayers of Tb and Gd adjacent to the NiFe and FeCo layers, respectively. Exploiting the antiferromagnetic coupling between the RE and TM layers, the small magnitudes of the damping, α, in the NiFe and FeCo layers, which initially are extremely close to each other, are evidently improved, resulting in a large difference between both values, namely $\alpha_{NiFe} \approx 2\alpha_{FeCo}$. The underlying mechanism of the observed increases in α has been unraveled, and can be chiefly ascribed to the enhanced orbital moments of Ni and Co, the spin and orbital moments of the RE, the lattice structure, and the electronic band structure of the TMs. In contrast, as a shared element in both NiFe and FeCo, the Fe shows little response to the RE insertions and thus gives only a tiny improvement in α. A practical method how to obtain the desired Gilbert damping in spin-valve trilayers has also been suggested, which would offer the opportunity toward realizing completely independent control of the magnetic damping, with a further systematic test and verification on more combinations of different RE and TM layers supplied. The present work will have clear significance for improving the performance of the aforementioned dual free-

DOI: 10.1021/acsami.5b03595
ACS Appl. Mater. Interfaces 2015, 7, 17070−17075

layer STOs by independently tuning the damping of the free layers. Different from some traditional STOs, where one TM layer serves as a free layer and the other as a fixed layer pinned by an antiferromagnetic layer, here both TM layers serve as free layers with two corresponding perpendicular polarizers, which are expected to offer a great improvement in microwave power emission.[17] Wider applications could be in devices based on the control of magnetization dynamics and their interplay with spin currents.

AUTHOR INFORMATION

Corresponding Authors

*E-mail: xiaotur@gmail.com.
*E-mail: yazhai@seu.edu.cn.

Notes

The authors declare no competing financial interest.

ACKNOWLEDGMENTS

We acknowledge the financial support from the National Natural Science Foundation of China for Young Scientists, Grant 61306121; China Postdoctoral Science Foundation, Grant 2013M541580; Natural Science Foundation of Jiangsu, Grant BK20141328. P.K.J.W. is financially supported by the EU FP7 Project SpinValley under Grant PIOF-GA-2013-628063.

REFERENCES

(1) Heinrich, B.; Bland, J. A. C. *Ultrathin Magnetic Structures IV*; Springer: Berlin, 2005.
(2) Baibich, M. N.; Broto, J. M.; Fert, A.; Van Dau, F. N.; Petroff, F.; Etienne, P.; Creuzet, G.; Friederich, A.; Chazelas, J. Giant Magnetoresistance of (001)Fe/(001)Cr Magnetic Superlattices. *Phys. Rev. Lett.* **1988**, *61*, 2472−2475.
(3) Yamamoto, H.; Motomura, Y.; Anno, T.; Shinjo, T. Magnetoresistance of Non-Coupled [NiFe/Cu/Co/Cu] Multilayers. *J. Magn. Magn. Mater.* **1993**, *126*, 437−439.
(4) Dieny, B.; Speriosu, V. S.; Gurney, B. A.; Parkin, S. S. P.; Wilhoit, D. R.; Roche, K. P.; Metin, S.; Peterson, D. T.; Nadimi, S. B. Spin-Valve Effect in Soft Ferromagnetic Sandwiches. *J. Magn. Magn. Mater.* **1991**, *93*, 101−104.
(5) Grünberg, P.; Schreiber, R.; Pang, Y.; Brodsky, M. B.; Sowers, H. Layered Magnetic Structures: Evidence for Antiferromagnetic Coupling of Fe Layers across Cr Interlayers. *Phys. Rev. Lett.* **1986**, *57*, 2442−2445.
(6) Stiles, M. D. Exchange Coupling in Magnetic Heterostructures. *Phys. Rev. B: Condens. Matter Mater. Phys.* **1993**, *48*, 7238−7258.
(7) Slonczewski, J. C. Mechanism of Interlayer Exchange in Magnetic Multilayers. *J. Magn. Magn. Mater.* **1993**, *126*, 374−379.
(8) Katine, J. A.; Albert, F. J.; Buhrman, R. A.; Myers, E. B.; Ralph, D. C. Current-Driven Magnetization Reversal and Spin-Wave Excitations in Co/Cu/Co Pillars. *Phys. Rev. Lett.* **2000**, *84*, 3149−3152.
(9) Bauer, G. E. W.; Brataas, A.; Tserkovnyak, Y.; van Wees, B. J. Spin-Torque Transistor. *Appl. Phys. Lett.* **2003**, *82*, 3928−3930.
(10) Kiselev, S. I.; Sankey, J. C.; Krivorotov, I. N.; Emley, N. C.; Schoelkopf, R. J.; Buhrman, R. A.; Ralph, D. C. Microwave Oscillations of a Nanomagnet Driven by a Spin-Polarized Current. *Nature* **2003**, *425*, 380−383.
(11) Urban, R.; Woltersdorf, G.; Heinrich, B. Gilbert Damping in Single and Multilayer Ultrathin Films: Role of Interfaces in Nonlocal Spin Dynamics. *Phys. Rev. Lett.* **2001**, *87*, 217204.
(12) Pelzl, J.; Meckenstock, R.; Spoddig, D.; Schreiber, F.; Pflaum, J.; Frait, Z. Spin-Orbit-Coupling Effects on *g*-Value and Damping Factor of the Ferromagnetic Resonance in Co and Fe Films. *J. Phys.: Condens. Matter* **2003**, *15*, S451−S463.
(13) Chikazumi, S. *Physics of Ferromagnetism*, 2nd ed.; Oxford University Press: Oxford, U.K., 2009; p 565.
(14) Gilbert, T. L. A Lagrangian Formulation of the Gyromagnetic Equation of the Magnetization Fields. *Phys. Rev.* **1955**, *100*, 1243.
(15) Suhl, H. Ferromagnetic Resonance in Nickel Ferrite between One and Two Kilomegacycles. *Phys. Rev.* **1955**, *97*, 555−557; Theory of the Magnetic Damping Constant. *IEEE Trans. Magn.* **1998**, *34*, 1834−1838.
(16) Heinrich, B.; Tserkovnyak, Y.; Woltersdorf, G.; Brataas, A.; Urban, R.; Bauer, G. E. W. Dynamic Exchange Coupling in Magnetic Bilayers. *Phys. Rev. Lett.* **2003**, *90*, 187601.
(17) Rowlands, G. E.; Krivorotov, I. N. Magnetization Dynamics in a Dual Free-Layer Spin-Torque Nano-Oscillator. *Phys. Rev. B: Condens. Matter Mater. Phys.* **2012**, *86*, 094425.
(18) Tserkovnyak, Y.; Brataas, A.; Bauer, G. E. W.; Halperin, B. I. Nonlocal Magnetization Dynamics in Ferromagnetic Heterostructures. *Rev. Mod. Phys.* **2005**, *77*, 1375−1421.
(19) Houssameddine, D.; Ebels, U.; Delaët, B.; Rodmacq, B.; Firastrau, I.; Ponthenier, F.; Brunet, M.; Thirion, C.; Michel, J.-P.; Prejbeanu-Buda, L.; Cyrille, M.-C.; Redon, O.; Dieny, B. Spin-Torque Oscillator Using a Perpendicular Polarizer and a Planar Free Layer. *Nat. Mater.* **2007**, *6*, 447−453.
(20) Kent, A. D.; Özyilmaz, B.; del Barco, E. Spin-Transfer-Induced Precessional Magnetization Reversal. *Appl. Phys. Lett.* **2004**, *84*, 3897.
(21) Brataas, A.; Tserkovnyak, Y.; Bauer, G. E. W.; Halperin, B. I. Spin Battery Operated by Ferromagnetic Resonance. *Phys. Rev. B: Condens. Matter Mater. Phys.* **2002**, *66*, 060404.
(22) Kambersky, V. On Ferromagnetic Resonance Damping in Metals. *Czech. J. Phys.* **1976**, *26*, 1366−1383.
(23) Sirvetz, M. H.; Zneimer, J. E. Microwave Properties of Polycrystalline Rare Earth Garnets. *J. Appl. Phys.* **1958**, *29*, 431−433.
(24) Bailey, W.; Kabos, P.; Mancoff, F.; Russek, S. Control of Magnetization Dynamics in Ni81Fe19(50nm) through the Use of Rare-Earth Dopants. *IEEE Trans. Magn.* **2001**, *37*, 1749−1751.
(25) Russek, S. E.; Kabos, P.; McMichael, R. D.; Lee, C. G.; Bailey, W. E.; Ewasko, R.; Sanders, S. C. Magnetostriction and Angular Dependence of Ferromagnetic Resonance Linewidth in Tb-Doped Ni0.8Fe0.2 Thin Films. *J. Appl. Phys.* **2002**, *91*, 8659−8661.
(26) Rebei, A.; Hohlfeld, J. Origin of Increase of Damping in Transition Metals with Rare-Earth-Metal Impurities. *Phys. Rev. Lett.* **2006**, *97*, 117601.
(27) Radu, I.; Woltersdorf, G.; Kiessling, M.; Melnikov, A.; Bovensiepen, U.; Thiele, J.-U.; Back, C. H. Laser-Induced Magnetization Dynamics of Lanthanide-Doped Permalloy Thin Films. *Phys. Rev. Lett.* **2009**, *102*, 117201.
(28) Ellis, M. O. A.; Ostler, T. A.; Chantrell, R. W. Classical Spin Model of the Relaxation Dynamics of Rare-Earth Doped Permalloy. *Phys. Rev. B: Condens. Matter Mater. Phys.* **2012**, *86*, 174418.
(29) Luo, C.; Feng, Z.; Fu, Y.; Zhang, W.; Wong, P. K. J.; Kou, Z. X.; Zhai, Y.; Ding, H. F.; Farle, M.; Du, J.; Zhai, H. R. Enhancement of Magnetization Damping Coefficient of Permalloy Thin Films with Dilute Nd Dopants. *Phys. Rev. B: Condens. Matter Mater. Phys.* **2014**, *89*, 184412.
(30) Zhang, W.; Jiang, S.; Wong, P. K. J.; Sun, L.; Wang, Y. K.; Wang, K.; de Jong, M. P.; van der Wiel, W. G.; van der Laan, G.; Zhai, Y. Engineering Gilbert Damping by Dilute Gd Doping in Soft Magnetic Fe Thin Films. *J. Appl. Phys.* **2014**, *115*, 17A308.
(31) Luo, C.; Zhang, W.; Wong, P. K. J.; Zhai, Y.; You, B.; Du, J.; Zhai, H. R. The Influence of Nd Dopants on Spin and Orbital Moments in Nd-Doped Permalloy Thin Films. *Appl. Phys. Lett.* **2014**, *105*, 082405.
(32) Hairston, D. K.; Kryder, M. H. The TM Dependence of the Magneto-Optic Signal in GdTb-TM Thin Films. *J. Appl. Phys.* **1988**, *63*, 3621−3623.
(33) Yang, T.; Matsumoto, T.; Yamane, H.; Kamiko, M.; Yamamoto, R. Perpendicular Magnetic Anisotropy and Magneto-Optical Properties of (Co-Tb)/Pd Multilayers. *J. Magn. Magn. Mater.* **1999**, *198*, 357−359.
(34) Kaiser, C.; Panchula, A. F.; Parkin, S. S. P. Finite Tunneling Spin Polarization at the Compensation Point of Rare-Earth-Metal-Transition-Metal Alloys. *Phys. Rev. Lett.* **2005**, *95*, 047202.

DOI: 10.1021/acsami.5b03595
ACS Appl. Mater. Interfaces 2015, 7, 17070−17075

(35) Maat, S.; Smith, N.; Carey, M. J.; Childress, J. R. Suppression of Spin Torque Noise in Current Perpendicular to the Plane Spin-Valves by Addition of Dy Cap Layers. *Appl. Phys. Lett.* **2008**, *93*, 103506.
(36) Marcham, M. K.; Keatley, P. S.; Neudert, A.; Hicken, R. J.; Cavill, S. A.; Shelford, L. R.; van der Laan, G.; Telling, N. D.; Childress, J. R.; Katine, J. A.; Shafer, P.; Arenholz, E. Phase-Resolved X-Ray Ferromagnetic Resonance Measurements in Fluorescence Yield. *J. Appl. Phys.* **2011**, *109*, 07D353.
(37) Heinrich, B.; Cochran, J. F.; Hasegawa, R. FMR Linebroadening in Metals due to Two-Magnon Scattering. *J. Appl. Phys.* **1985**, *57*, 3690−3692.
(38) Urban, R.; Heinrich, B.; Woltersdorf, G.; Ajdari, K.; Myrtle, K.; Cochran, J. F.; Rozenberg, E. Nanosecond Magnetic Relaxation Processes in Ultrathin Metallic Films Prepared by MBE. *Phys. Rev. B: Condens. Matter Mater. Phys.* **2001**, *65*, 020402.
(39) Heinrich, B.; Cochran, J. F. Ultrathin Metallic Magnetic Films: Magnetic Anisotropies and Exchange Interactions. *Adv. Phys.* **1993**, *42*, 523−639.
(40) McMichael, R. D.; Twisselmann, D. J.; Kunz, A. Localized Ferromagnetic Resonance in Inhomogeneous Thin Films. *Phys. Rev. Lett.* **2003**, *90*, 227601.
(41) Zhang, W.; Morton, S. A.; Wong, P. K. J.; Lu, B.; Xu, Y. B.; de Jong, M. P.; van der Wiel, W. G.; van der Laan, G. Microscopic Origin of the Reduced Magnetocrystalline Anisotropy with Increasing Oxide Content in Co80Pt20:Oxide Thin Films. *J. Phys. D: Appl. Phys.* **2013**, *46*, 405001.
(42) Zhang, W.; Morton, S. A.; Wong, P. K. J.; Hu, X. F.; Arenholz, E.; Lu, B.; Cheng, T. Y.; Xu, Y. B.; van der Laan, G. Magnetocrystalline Anisotropy of Magnetic Grains in Co80Pt20:Oxide Thin Films Probed by X-Ray Magnetic Circular Dichroism. *J. Appl. Phys.* **2011**, *109*, 113920.
(43) Thole, B. T.; Carra, P.; Sette, F.; van der Laan, G. X-Ray Circular Dichroism as a Probe of Orbital Magnetization. *Phys. Rev. Lett.* **1992**, *68*, 1943−1946.
(44) van der Laan, G.; Figueroa, A. I. X-Ray Magnetic Circular Dichroism - a Versatile Tool to Study Magnetism. *Coord. Chem. Rev.* **2014**, *277*−*278*, 95−129.
(45) Brooks, M. S. S.; Eriksson, O.; Johansson, B. 3*d*-5*d* Band Magnetism in Rare Earth Transition Metal Intermetallics: LuFe. *J. Phys.: Condens. Matter* **1989**, *1*, 5861−5874.
(46) Brooks, M. S. S.; Nordstrom, L.; Johansson, B. Rare-Earth Transition-Metal Intermetallics. *Phys. B* **1991**, *172*, 95−100.
(47) Jaouen, N.; Tonnerre, J. M.; Raoux, D.; Bontempi, E.; Ortega, L.; Münzenberg, M.; Felsch, W.; Rogalev, A.; Dürr, H. A.; Dudzik, E.; van der Laan, G.; Maruyama, H.; Suzuki, M. Ce 5*d* Magnetic Profile in Fe/Ce Multilayers for the α and γ-Like Ce Phases by X-Ray Resonant Magnetic Scattering. *Phys. Rev. B: Condens. Matter Mater. Phys.* **2002**, *66*, 134420.
(48) Tyer, R.; van der Laan, G.; Temmerman, W. M.; Szotek, Z.; Ebert, H. Systematic Theoretical Study of the Spin and Orbital Magnetic Moments of 4*d* and 5*d* interfaces with Fe films. *Phys. Rev. B: Condens. Matter Mater. Phys.* **2003**, *67*, 104409.
(49) Woltersdorf, G.; Kiessling, M.; Meyer, G.; Thiele, J.-U.; Back, C. H. Damping by Slow Relaxing Rare Earth Impurities in Ni80Fe20. *Phys. Rev. Lett.* **2009**, *102*, 257602.
(50) Reidy, S. G.; Cheng, L.; Bailey, W. E. Dopants for Independent Control of Precessional Frequency and Damping in Ni81Fe19 (50 nm) Thin Films. *Appl. Phys. Lett.* **2003**, *82*, 1254−1256.
(51) Bailey, W. E.; Song, H.; Cheng, L. XMCD Characterization of Rare-Earth Dopants in Ni81Fe19 (50nm): Microscopic Basis of Engineered Damping. arXiv:cond-mat/0403627.
(52) van der Laan, G. Microscopic Origin of Magnetocrystalline Anisotropy in Transition Metal Thin Films. *J. Phys.: Condens. Matter* **1998**, *10*, 3239−3253.

DOI: 10.1021/acsami.5b03595
ACS Appl. Mater. Interfaces 2015, 7, 17070−17075